Time-resolved measurements of surface spin-wave pulses at millikelvin temperatures

A. F. van Loo,[1,*] R. G. E. Morris,[1] and A. D. Karenowska[1]

[1] *Clarendon Laboratory, Department of Physics, University of Oxford, OX1 3PU Oxford, United Kingdom*

(Dated: October 27, 2016)

In this work, we experimentally investigate the propagation of pulsed magnetostatic surface spin-wave (magnon) signals in an yttrium iron garnet (YIG) waveguide at millikelvin temperatures. Our measurements are performed in a dilution refrigerator at microwave frequencies. The excellent signal-to-noise ratio afforded by the low-temperature environment allows the propagation of the pulses to be observed in detail. The work gives insight both into low-temperature magnon dynamics in YIG and the potential application of systems of propagating magnons to solid-state quantum information processing.

arXiv:1610.08402v1 [cond-mat.mes-hall] 26 Oct 2016

The unusual and highly-tunable dispersion of propagating magnons in yttrium iron garnet ($Y_3Fe_5O_{12}$, YIG) has recently excited the interest of the superconducting circuit quantum electrodynamics (QED) community. The frequencies at which superconducting quantum devices typically operate overlap with the band in which magnons can be excited in YIG and, as superconducting quantum bit (qubit) structures are generally sensitive to electromagnetic fields, magnons and superconducting qubits can be made to communicate. So far, magnons in spheres of YIG have been shown to couple strongly to 3D cavities [1–4], reentrant cavities [5, 6] and to superconducting qubits via such cavities [7]. Furthermore, magnons in YIG films have been shown to interact with superconducting coplanar waveguides and 3D resonators [8, 9].

In this work, we investigate the propagation of magnetostatic surface magnons in a YIG waveguide made from a high-purity monocrystalline film grown by liquid phase epitaxy on a gallium gadolinium garnet (GGG) substrate. Our measurements are performed in a dilution refrigerator at temperatures of ∼10 mK, where thermal excitations of GHz-frequency magnons and photons are negligible. We previously investigated a similar system in [10], focusing on achieving signal limits equivalent to the propagation of single magnons. In this paper, we study the propagation of the excitations in significantly greater detail, comparing our experimental measurements with the predictions of theory. A thorough understanding of low temperature magnon propagation is an essential step towards the integration of systems of propagating magnons with circuit QED systems. Work in this area sets its sights not only on the development of new quantum devices, but also the use of the sophisticated technology and methods developed for superconducting quantum computing to investigate the quantum mechanics of single magnons.

In order to excite propagating magnons in a waveguide, a magnetic bias field must be applied. The dynamics of the particular modes which can be observed depend on the orientation of the bias field relative to the waveguide axis: in this study, we focus on magnetostatic surface spin waves (MSSW, also called Damon-Eshbach modes) which propagate when the field is in plane, across the width of the waveguide.

The dispersion relation for MSSW [11] can be written

$$\omega = \sqrt{\omega_H\left(\omega_H + \omega_M\right) + \frac{\omega_M^2}{4}\left(1 - \mathrm{e}^{-2kd}\right)} \tag{1}$$

where $\omega_M = -\gamma\mu_0 M_\mathrm{S}$ and $\omega_H = -\gamma B$. Here, d is the film thickness, γ is the gyromagnetic ratio, μ_0 is the vacuum permeability, B is the applied magnetic field, and M_S the saturation magnetization ($197.4\,\mathrm{kA\,m^{-1}}$ in our film at ∼10 mK). From the dispersion relation, the group and phase velocities (v_gr and v_ph respectively) can be derived:

$$v_\mathrm{gr} = \frac{\partial\omega}{\partial k} = \frac{d\left((2\omega_H + \omega_M)^2 - 4\omega^2\right)}{4\sqrt{\omega^2}} \tag{2}$$

$$v_\mathrm{ph} = \frac{\omega}{k} = \frac{-2d\sqrt{\omega^2}}{\log\left[\frac{(-2\omega+2\omega_H+\omega_M)(2(\omega+\omega_H)+\omega_M)}{\omega_M^2}\right]} \tag{3}$$

The YIG waveguide used in our experiments is 9 μm thick, 2 mm wide, and approximately 15 mm long. To prevent coherent reflections of spin waves from the ends, both are cleaved at a 45 degree angle. The waveguide is affixed to a PCB in close contact with two lithographed stripline antennae (Fig. 1a) which are 50 μm wide and 6 mm apart. The complete assembly is housed in a copper sample box attached to the cold plate of a dilution refrigerator. A superconducting magnet is connected to the 4 K plate of the refrigerator and positioned such that the homogeneity of the field it produces is maximal at the position of the waveguide. The orientation of the field relative to the waveguide (Fig. 1a) is such that only surface spin waves (MSSW) are excited. Due to the non-reciprocal nature of these excitations, they are only able to travel in one direction: from the input port to the output port of the experiment [11, 12].

To ensure that room-temperature noise cannot couple into the waveguide, the line connected to the input antenna is heavily attenuated inside the refrigerator (Fig. 2). The output antenna is connected to a

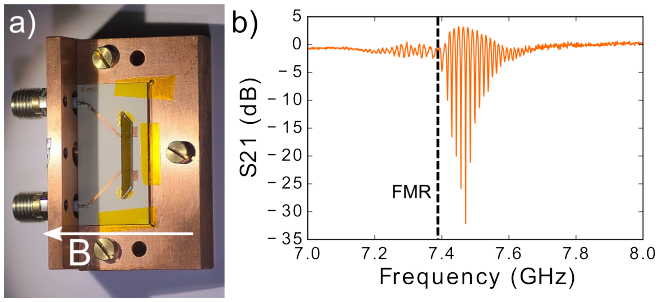

FIG. 1. (a) The YIG waveguide is attached to a PCB with two inductive antennae on its surface (an input and an output). The complete experimental assembly is housed in a copper box attached to the cold plate of a dilution refrigerator. (b) Measured transmission of a continuous-wave signal through the sample in a magnetic bias field of 167 mT. The dashed line indicates the position of the ferromagnetic resonance frequency.

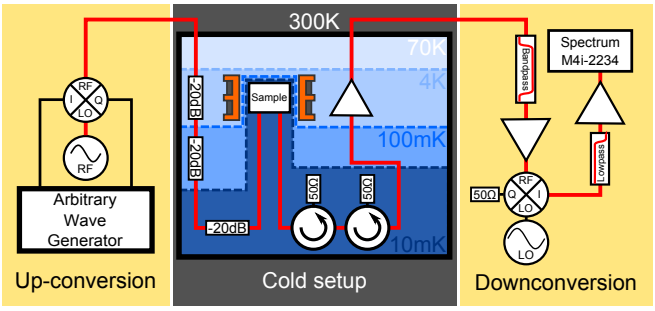

FIG. 2. The microwave setup used in our experiments can be divided into three parts. In the up-conversion section, short microwave pulses are created by mixing the output of a continuous-wave microwave source with envelope shapes generated by an AWG. Inside the dilution refrigerator, the input line to the sample is heavily attenuated to thermalize the signal, such that the electronic noise temperature is decreased to a level similar to the phonon noise temperature. The down-conversion system allows for the recovery of the envelope of the signal transmitted through the waveguide.

low-temperature HEMT amplifier via two isolators. The amplified signal is filtered and down-converted to an intermediate frequency of 500 MHz at room temperature. A fast data acquisition card (Spectrum M4i-2234-x8) records the resulting voltage as a function of time at a rate of 2.5 GHz for 800 ns. Typically 2,000 to 40,000 such traces are recorded and averaged, though much higher numbers are can be used if desired (e.g. when the input signal is reduced to very low levels). Through this step, incoherent and inelastically scattered signals cancel out, leaving only the coherently scattered radiation at the drive frequency. After a digital down-conversion and filtering step, the envelope of the transmitted microwave signal is recovered.

When a microwave-frequency signal is applied to the input antenna, there are two routes by which it can reach the output: via the vacuum in the sample box as microwave photons at the speed of light c, and as MSSW in the magnetic waveguide at the group velocity determined by eq. 2. The MSSW group velocity is typically several orders of magnitude slower than c.

To perform an initial characterization of the YIG film, we connect the cold setup (center part of Fig. 2) to a network analyzer, and measure the transmission (S21) of the experimental system between 4 and 8 GHz. Data from such a measurement are shown in Fig. 1b. The low-frequency limit of the magnon passband is the ferromagnetic resonance (FMR) frequency (around 7.4 GHz in the figure); this is the $k = 0$ mode of the magnon system in which the spins throughout the sample precess in phase. The oscillations in the signal transmittance as a function of frequency is caused by interference between the vacuum and magnon signals.

Having performed our initial characterization in the continuous-wave regime, we investigate the dynamics of the magnetic system by driving it with short microwave pulses. Advantageously, since the propagation velocity of the vacuum signal greatly exceeds that of the magnons in the YIG film, the two signals become fully separated in time for pulsed excitations of sufficiently short duration. Such time-resolved measurements also allow for the investigation of different magnetostatic surface spin-wave modes (i.e. those with different wave numbers) at a single magnetic field and frequency. Figure 2 shows the experimental setup used to generate and measure the transmittance of short microwave pulses through the YIG sample.

Figure 3a shows the spin-wave output signal in response to the application of a square 30 ns microwave pulse of constant carrier frequency (7.9 GHz) as the magnetic bias field is swept across the magnon band. Sweeping the magnet current at fixed drive frequency eliminates the effect of the frequency-dependent attenuation of the microwave lines and components on the data. The horizontal stripe of high signal intensity from 0 to 30 ns is the vacuum signal (i.e. due to direct electromagnetic interaction between the two antennae). The magnon signal begins to appear at $\sim$ 75 ns. The field at which FMR occurs is 182 mT. When the field is reduced below that corresponding to the FMR frequency (moving from right to left along the horizontal axis of the figure), the drive frequency excites modes of increasingly higher k which have a lower group velocity (Eq. 2) and therefore take longer to reach the output antenna. The progressive weakening of the magnon signal as the field is further decreased occurs due to the reduction in the coupling of the input and output antennae to the magnon system at higher values of k (or smaller wavelengths) as this coupling is proportional to the overlap between the magnon field and the field due to the antenna.

Figure 3b shows the results of a simulation of the response of the experimental system calculated based on Eq. 1. These calculations are made as follows: The sim-

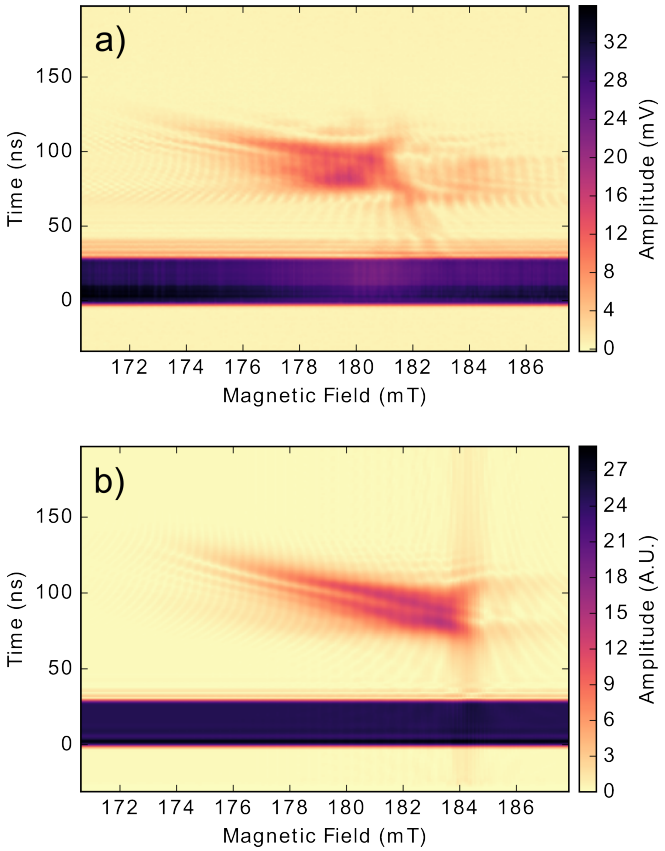

FIG. 3. Measurements and simulations of pulsed propagating magnon signals. (a) Experimental data showing the transmitted signal amplitude due to a square 30 ns microwave pulse with a carrier frequency of 7.9 GHz. The magnetic bias field (horizontal axis) is swept across the magnon band. (b) Results of a simulation under the same conditions assuming ideal antennae and sample box. The $\sim$ 3mT difference in the FMR frequency (right edge of the magnon response) is thought to be due to a small difference between the current set on the current source and used in the calculations, and the actual current flowing through the magnet in experiment.

ulated input signal is an ideal version of the real signal, that is, a microwave frequency carrier tone with a 30 ns square pulse envelope and with a small offset to account for imperfect mixer calibration. This input signal is Fourier transformed, and for each frequency component, the phase velocity is calculated. The arrival time of each frequency component at the output antenna is then determined from the phase velocity and the distance between the antennae. The time-dependent signal is reconstructed via an inverse Fourier transform, after which the processes of filtering and down-conversion are mimicked. To avoid over-fitting, the antennae and sample box are treated as being ideal, save a k-dependent coupling factor between the antennae and the YIG, obtained from the antenna geometry. The ratio between antenna-yig coupling and antenna-antenna coupling is set manually to resemble the data.

As predicted by eq. 2, the speed of the magnons reduces as their wavenumber increases, resulting in an upwards curve of the magnon signal on the left side of both panels of Fig. 3. It can be seen that there is very good agreement between experiment and theory, especially regarding the structure and shape of the magnon response to the left of the FMR field in the plot. There are, however, also some differences which warrant discussion.

One difference between simulation and experiment is the vertical line close to the FMR frequency only seen in the theoretical plot. This line is an artefact of the simulation that comes about from the phase velocity tending to infinity as k reduces to zero. In the real physical system, the phase velocity diverges close to the FMR frequency producing a signal between the magnon pulse and the direct-coupled signal. We also see some ringing in the experiments which is not reproduced in the data; this occurs as a result of unmodeled nonidealities of the antennae and samplebox. A further difference exists to right of the FMR: in Fig. 3a there is a structure in the measurement which is not reproduced in the simulations. This signal disappears when the magnetic bias field is reversed, confirming it must be due to a surface mode rather than a (reciprocal) backward or forward volume excitation. From further calculations, it also seems unlikely that this signal is due to the finite width of the waveguide [13], inhomogeneity of the applied magnetic bias field, or effects due to the presence of a ground plane close to the sample [14]. A possible explanation for this phenomenon is that the inhomogeneous magnetic fields close to the edges of the waveguide causes localised modes [15]. It should be noted that evidence of this signal is also found in the continuous-wave experiment (to the left of the FMR line in Fig. 1b).

Our microwave setup can be used to inject pulses of arbitrary envelope into the experimental system. In Fig. 4a, we see the output signal in response to a Gaussian input with $\sigma = 12$ ns, and in Fig. 4b, a train of three 20 ns pulses separated by 10 ns. In the latter figure, the signal produced by the direct coupling of the last of the input pulses from the input antenna to the output antenna overlaps with the first magnon pulse. The result is an interference pattern akin to that seen in Fig. 1b. The excellent definition of the individual pulses in the train underlines the promising potential of magnon systems as a platform for the transmission of information signals.

In conclusion, in this work we present a detailed study of the propagation of pulsed magnetostatic surface spin-wave signals in an yttrium iron garnet waveguide at millikelvin temperatures. Calculations using a simple model based on the dispersion relation of MSSW agree well with our experimental findings. Our investigations confirm that trains of short spin-wave pulses can readily be excited and detected inductively in YIG waveguides grown on gallium gadolinium substrates. As well as being of interest in their own right, these results are an important

step towards the combination of systems of propagating magnons with microwave superconducting quantum circuit technology.

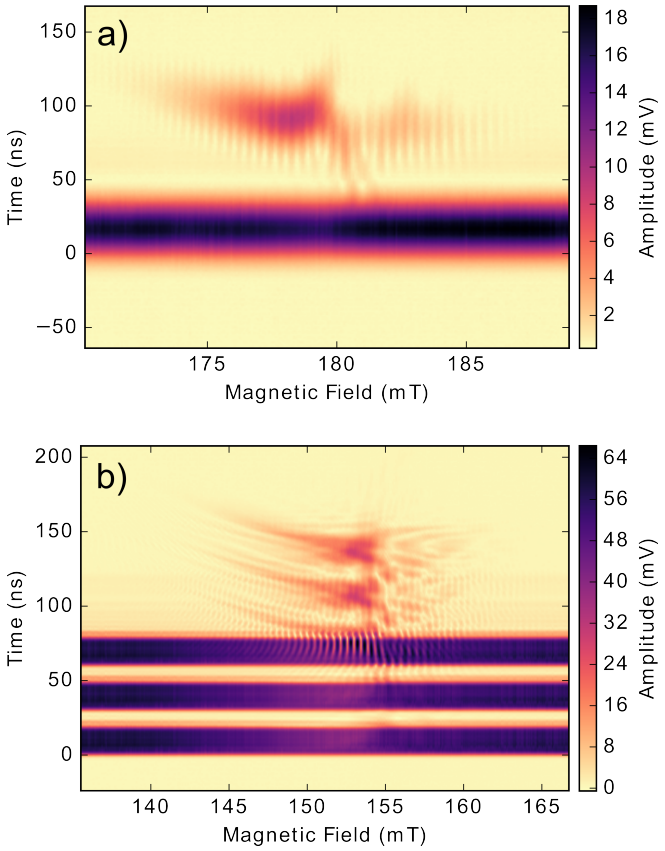

FIG. 4. (a) A Gaussian pulse with a sigma of 12 ns. (b) A train of 20 ns pulses separated by 10 ns.

The authors would like to acknowledge Bob Watkins for preparing the waveguide and the EPSRC for funding this research with grant EP/K032690/1.

* arjan.vanloo@physics.ox.ac.uk

[1] Y. Tabuchi, S. Ishino, T. Ishikawa, R. Yamazaki, K. Usami, and Y. Nakamura, *"Hybridizing ferromagnetic magnons and microwave photons in the quantum limit,"* Phys. Rev. Lett. **113**, 083603 (2014).

[2] J. Bourhill, N. Kostylev, M. Goryachev, D. L. Creedon, and M. E. Tobar, *"Ultrahigh cooperativity interactions between magnons and resonant photons in a yig sphere,"* Phys. Rev. B **93**, 144420 (2016).

[3] X. Zhang, C.-L. Zou, L. Jiang, and H. X. Tang, *"Strongly coupled magnons and cavity microwave photons,"* Phys. Rev. Lett. **113**, 156401 (2014).

[4] D. Zhang, X.-M. Wang, T.-F. Li, X.-Q. Luo, W. Wu, F. Nori, and J. Q. You, *"Cavity quantum electrodynamics with ferromagnetic magnons in a small yttrium-iron-garnet sphere,"* Npj Quantum Inf. **1**, 15014 (2015).

[5] M. Goryachev, W. G. Farr, D. L. Creedon, Y. Fan, M. Kostylev, and M. E. Tobar, *"High-cooperativity cavity qed with magnons at microwave frequencies,"* Phys. Rev. Applied **2**, 054002 (2014).

[6] N. Kostylev, M. Goryachev, and M. E. Tobar, *"Superstrong coupling of a microwave cavity to yttrium iron garnet magnons,"* Appl. Phys. Lett. **108**, 062402 (2016), http://dx.doi.org/10.1063/1.4941730.

[7] Y. Tabuchi, S. Ishino, A. Noguchi, T. Ishikawa, R. Yamazaki, K. Usami, and Y. Nakamura, *"Coherent coupling between a ferromagnetic magnon and a superconducting qubit,"* Science (2015), 10.1126/science.aaa3693.

[8] H. Huebl, C. W. Zollitsch, J. Lotze, F. Hocke, M. Greifenstein, A. Marx, R. Gross, and S. T. B. Goennenwein, *"High cooperativity in coupled microwave resonator ferrimagnetic insulator hybrids,"* Phys. Rev. Lett. **111**, 127003 (2013).

[9] X. Zhang, C. Zou, L. Jiang, and H. X. Tang, *"Superstrong coupling of thin film magnetostatic waves with microwave cavity,"* J. Appl. Phys. **119**, 023905 (2016), http://dx.doi.org/10.1063/1.4939134.

[10] A. D. Karenowska, A. D. Patterson, M. J. Peterer, E. B. Magnússon, and P. J. Leek, *"Excitation and detection of propagating spin waves at the single magnon level,"* arXiv:1502.06263 (2015).

[11] B. A. Kalinikos, *"Spectrum and linear excitation of spin waves in ferromagnetic films,"* Sov. Phys. J. **24**, 718 (1981).

[12] A. Gurevich and G. Melkov, *Magnetization Oscillations and Waves* (CRC Press, Inc, 1996).

[13] T. W. O'Keeffe and R. W. Patterson, *"Magnetostatic surface-wave propagation in finite samples,"* J. Appl. Phys. **49**, 4886 (1978).

[14] T. Yukawa, J. ichi Yamada, K. Abe, and J. ichi Ikenoue, *"Effects of metal on the dispersion relation of magnetostatic surface waves,"* Jpn. J. Appl. Phys. **16**, 2187 (1977).

[15] K. Y. Guslienko, R. W. Chantrell, and A. N. Slavin, *"Dipolar localization of quantized spin-wave modes in thin rectangular magnetic elements,"* Phys. Rev. B **68**, 024422 (2003).